[10] J. Shi, M. Cracraft, K. Slattery, M. Yamaguchi, and R. DuBroff, "Calibration and compensation of near-field scan measurements," *IEEE Trans. Electromagn. Compat.*, vol. 47, no. 3, pp. 642–650, Aug. 2005.
[11] S. Burgos, S. Pivnenko, O. Breinbjerg, and M. Sierra-Castañer, "Comparative investigation of four antenna gain determination techniques," in *Proc. 2nd Eur. Conf. on Antennas and Propagation, EuCAP*, Nov. 2007, pp. 1–6.

A Modified Wheeler Cap Method for Efficiency Measurements of Probe-Fed Patch Antennas With Multiple Resonances

Chihyun Cho, Ikmo Park, and Hosung Choo

***Abstract*—We propose a modified Wheeler cap method to accurately measure the radiation efficiency of patch antennas with multiple resonances by modeling their impedance as a high-order circuit model. The radiation efficiency is obtained from the power consumption ratio between the radiation and loss conductances using a circuit model we developed. Our technique is validated by measuring the efficiencies of a circularly polarized microstrip patch antenna and a triple-band microstrip patch antenna. The measurement results are in close agreement with those produced by simulations, whereas the Wheeler cap method with a series-(or parallel-) resonant circuit model is shown to be unreliable.**

***Index Terms*—Antenna efficiency, circuit model, Wheeler cap.**

I. Introduction

There are various methods for measuring radiation efficiency, such as methods using a near-field, a reverberation chamber, a calorimetric scheme, and a Wheeler cap [1]–[4]. Among these methods, the Wheeler cap method is the most widely used technique for measuring small antennas because of its simple procedure and reasonably good accuracy [4]–[10]. It is based on the assumption that the antenna operates as a simple parallel (or series) circuit, and the efficiency is measured by comparing the input conductances (or resistances) of the antenna in free space and inside the Wheeler cap. However, if a microstrip antenna has multimode frequency characteristics (such as circularly polarized radiation), multiple frequency resonances, or coupled resonances using a sub-radiator, the Wheeler cap method with a series-(or parallel-) resonant circuit model produces unreliable results because the operation of such an antenna cannot be represented as a simple parallel (or series) resonance circuit.

Manuscript received May 26, 2009; revised January 22, 2010; accepted March 19, 2010. Date of publication June 14, 2010; date of current version September 03, 2010. This work was supported by the Ministry of Knowledge Economy (MKE), Korea, under the Information Technology Research Center (ITRC) support program supervised by the Institute for Information Technology Advancement (IITA) (IITA-2009-C1090-0904-0002).

C. Cho is with the Institute of Advanced Technologies, Samsung Thales, Yongin, Korea.
I. Park is with the Department of Electrical and Computer Engineering, Ajou University, Suwon, Korea.
H. Choo is with the School of Electronic and Electrical Engineering, Hongik University, Seoul, Korea (e-mail: hschoo@hongik.ac.kr).

Color versions of one or more of the figures in this communication are available online at http://ieeexplore.ieee.org.
Digital Object Identifier 10.1109/TAP.2010.2052553

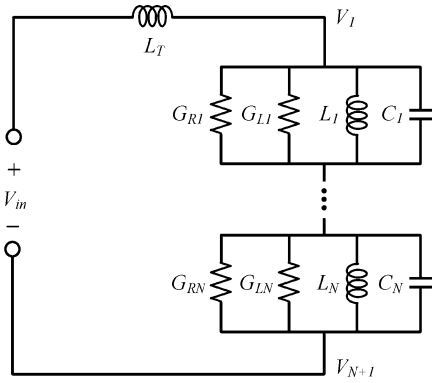

Fig. 1. Proposed equivalent circuit model for probe-fed microstrip patch antennas with multimode operation using the Wheeler cap method.

In this communication, we introduce a modified Wheeler cap method using a high-order circuit model to obtain more accurate efficiency measurements for probe-fed microstrip patch antennas. To validate our technique, we measured the radiation efficiency of a microstrip antenna with circularly polarized radiation and a miniaturized triple-band patch antenna. The results are compared to measurements made using the Wheeler cap method with a series-(or parallel-) resonant circuit model and to those of a simulator.

II. Methodology

To obtain a more accurate estimate for the efficiency of a multimode microstrip antenna, we use a high-order circuit model in the Wheeler cap method. Specifically, a cascade form of parallel resonance circuits is used to represent the frequency characteristics of the microstrip patches more precisely [11]–[13]. In this model, we separate each conductance into a radiation conductance (G_{Rn}) and a loss conductance (G_{Ln}), as illustrated in Fig. 1. The input impedance $Z_{\rm in}$ of the model is then given by

$$Z_{\rm in} = \frac{1}{G_{R1}+G_{L1}+\frac{1}{j\omega L_1}+j\omega C_1}+\cdots + \frac{1}{G_{RN}+G_{LN}+\frac{1}{j\omega L_N}+j\omega C_N}+j\omega L_T. \quad (1)$$

Equation (1) can be separated into real and imaginary components, as follows:

$$\begin{aligned} Z_{\rm in} &= R_{\rm in}+jX_{\rm in} \\ &= \sum_{n=1}^{N}\left(\frac{\omega L_n(\omega L_n G_{Tn})}{(\omega L_n G_{Tn})^2+(1-\omega^2 L_n C_n)^2}\right) \\ &\quad + j\sum_{n=1}^{N}\left(\frac{\omega L_n(1-\omega^2 L_n C_n)}{(\omega L_n G_{Tn})^2+(1-\omega^2 L_n C_n)^2}+\omega L_T\right) \end{aligned} \quad (2)$$

where

$$G_{Tn} = G_{Rn}+G_{Ln}.$$

Unlike the single parallel (or series) circuit used in the conventional Wheeler cap method, the total input power and the radiated power in the model represented by (2) cannot be separated by simply comparing

TABLE I
LUMPED ELEMENT VALUES OF THE EQUIVALENT CIRCUIT MODEL FOR THE CP MICROSTRIP PATCH ANTENNA

	L_t (nH)	G_1 (mS)	L_1 (nH)	C_1 (pF)	G_2 (mS)	L_2 (nH)	C_2 (pF)
Free space	2.6	20.8333	0.23	140.9314	38.4615	0.17	176.0418
In the cap	2.6	16.3934	0.23	137.4885	28.9855	0.17	172.2763

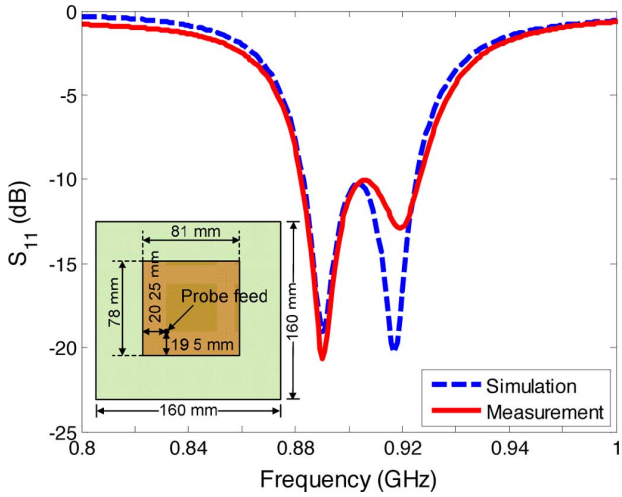

Fig. 2. Simulated (- - - - -) and measured (——) reflection coefficient of the CP microstrip patch antenna and a photo of the actual antenna.

the input conductances in free space and in the cap because the measured input impedance is influenced by multiple conductances. To obtain an accurate estimate for the efficiency, we must therefore find the appropriate lumped element values of the model, and then extract the radiation efficiency by calculating the power consumption in each conductance of the circuit.

We derived simultaneous equations from (2) to determine these lumped values. At least $3N + 1$ simultaneous equations are required, since this is the number of unknown lumped values $(G_{T1}, \ldots, G_{Tn}, L_1, \ldots, L_n, C_1, \ldots, C_n, L_T)$. These equations can be constructed by using $k(\geq 3N + 1)$ frequency points in the impedance measurements, as in (3) and (4). Equations (5) and (6) can be constructed in a like manner, for the case when the antenna is shielded by the Wheeler cap. We are assuming that the Wheeler cap shielding completely eliminates the radiation conductance G_{Rn}, so that the conductance G_{Tn} is reduced to G_{Ln}. The solutions for the lumped element values $(G_{T1}, \ldots, G_{Tn}, G_{L1}, \ldots, G_{Ln}, L_1, \ldots, L_n, C_1, \ldots, C_n, L_T)$ can be obtained from (3)–(6) in various ways, including iterative methods, global optimization techniques, or trial and error

$$G_{\text{in}}^{\text{free-space}}(\omega_1, \ldots, \omega_k) = \sum_{n=1}^{N} \left(\frac{\left(\omega_{(1,\ldots,k)} L_n G_{Tn}\right)^2 + \left(1 - \omega_{(1,\ldots,k)}^2 L_n C_n\right)^2}{\omega_{(1,\ldots,k)} \left(L_n \omega_{(1,\ldots,k)} L_n G_{Tn}\right)} \right) \quad (3)$$

$$B_{\text{in}}^{\text{free-space}}(\omega_1, \ldots, \omega_k) = -1 / \sum_{n=1}^{N} \frac{\omega_{(1,\ldots,K)} L_n \left(1 - \omega_{(1,\ldots,k)}^2 L_n C_n\right)}{\left(\omega_{(1,\ldots,k)} L_n G_{Tn}\right)^2 + \left(1 - \omega_{(1,\ldots,k)}^2 L_n C_n\right)^2} + \omega_{(1,\ldots,k)} L_T \quad (4)$$

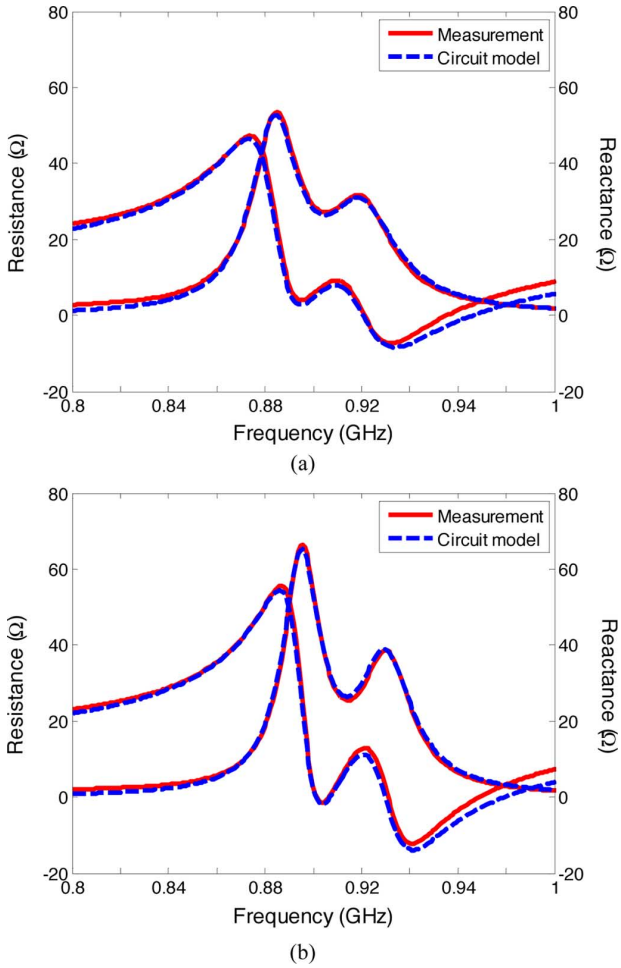

Fig. 3. Calculated impedance of the equivalent circuit (- - - - -) and measured impedance (——) for the CP microstrip patch antenna (a) in free space and (b) in the cap.

$$G_{\text{in}}^{\text{cap}}(\omega_1, \ldots, \omega_k) = \sum_{n=1}^{N} \left(\frac{\left(\omega_{(1,\ldots,k)} L_n G_{Ln}\right)^2 + \left(1 - \omega_{(1,\ldots,k)}^2 L_n C_n\right)^2}{\omega_{(1,\ldots,k)} \left(L_n \omega_{(1,\ldots,k)} L_n G_{Ln}\right)} \right) \quad (5)$$

$$B_{\text{in}}^{\text{cap}}(\omega_1, \ldots, \omega_k) = -1 / \sum_{n=1}^{N} \frac{\omega_{(1,\ldots,K)} L_n \left(1 - \omega_{(1,\ldots,k)}^2 L_n C_n\right)}{\left(\omega_{(1,\ldots,k)} L_n G_{Ln}\right)^2 + \left(1 - \omega_{(1,\ldots,k)}^2 L_n C_n\right)^2} + \omega_{(1,\ldots,k)} L_T. \quad (6)$$

The resulting circuit model should be able to represent the input impedance of the antenna under test (AUT) in free space, as well as in the cap. This means that the input impedance of the AUT in the Wheeler cap should be modeled by using its free-space circuit model

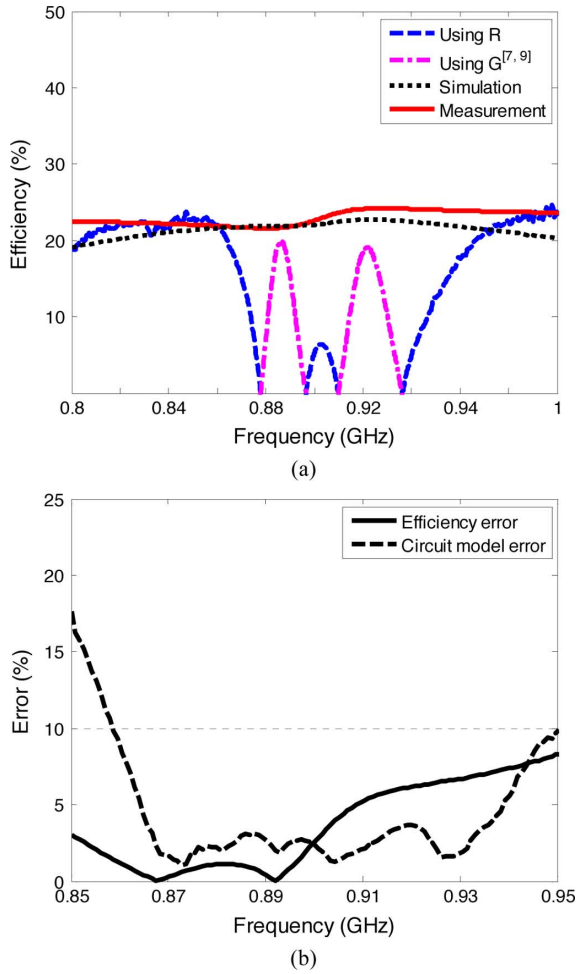

Fig. 4. Measured results for the CP microstrip patch antenna. (a) Efficiency measured by the proposed method (——) and the conventional Wheeler cap method using R comparison (- - - - -) and G comparison (—·—·—), and the simulated results (· · · · · · ·). (b) Efficiency error between the proposed method and the simulation (——) and impedance error between the equivalent circuit and the measured values (- - - - -).

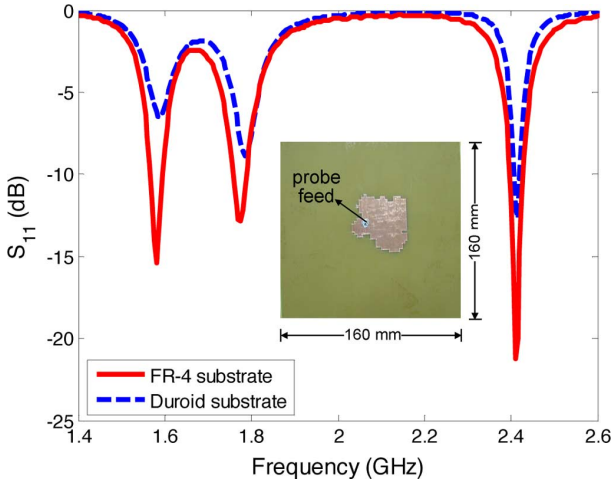

Fig. 5. Measured reflection coefficient of the miniaturized multi-resonance antennas using GA [8] on the FR-4 (——) and Duroid (- - - - -) substrates.

only, changing the conductance values (G_{Tn}) while keeping the inductors (L_n) and capacitors (C_n) the same. Thus, the radiation conductances G_{Rn} can be found by comparing G_{Tn} of the free-space circuit and G_{Ln} of the shielded model for the cap. Finally, the radiation efficiency can be calculated from the power consumption of the distributed conductances via (7)

$$\text{Efficiency} = \frac{\sum_{n=1}^{N} |V_n - V_{n+1}|^2 G_{Rn}}{\sum_{n=1}^{N} |V_n - V_{n+1}|^2 (G_{Rn} + G_{Ln})}. \quad (7)$$

However, the complexity and the time of solving each circuit element drastically increase as the number of circuits N grows. Thus, in this communication, to lessen the circuit-building procedure's complexity and optimization time, we restricted our method to patch antennas that had fewer than four clean resonances.

III. Measured Results

A. *Efficiency of a CP Microstrip Patch Antenna*

To verify the accuracy of the procedure, we measured the efficiency of a commonly used circularly polarized microstrip patch. The antenna has a substrate (FR-4, $\varepsilon_r = 4.2$, $\tan\delta = 0.02$) thickness of 1.6 mm, a patch size of 81 mm × 78 mm, and a probe feed located 20.25 mm and 19.5 mm from the respective edges, as shown in the inset of Fig. 2. In the same figure, the simulated result using an IE3D EM Simulator (dashed line) is in close agreement with the actual measurement (solid line) [14]. The antenna has two resonances in the vicinity, with circularly polarized radiation occurring in the middle of the two resonances. We used the circuit model shown in Fig. 1, with two parallel circuits ($N = 2$) to model the double resonance of the antenna and calculated the lumped element values listed in Table I. Each lumped values was found by fitting data from the measured input impedance. To lessen the complexity in the circuit building procedures, we set C_1 and C_2 to resonate at 884 MHz and 920 MHz, respectively. The two capacitances are calculated using (8), and they produce two peaks in the shape of the resistance response of the circuit model

$$C_n = \frac{1}{(2\pi f_n)^2 L_n}. \quad (8)$$

Fig. 3(a) shows the measured input impedance (solid line) and the calculated impedance (dashed line) using the free-space circuit model. For the Wheeler cap, we used a rectangular cavity (160 mm × 160 mm × 50 mm) made of copper. The resulting input impedances with the cap are also shown in Fig. 3(b). The calculated input resistance and the reactance predicted by the circuit model are both close to the actual measurements. As expected, the conductance values inside the cap are less than those in free space, and the decreased conductance is due to the elimination of radiation conductance by the shielding of the cap. When the Wheeler cap is placed onto the antenna, the two input resistance peaks are shifted from 884–895 MHz and from 920–930 MHz, and thus the capacitance values also change slightly by 3.4 pF and 3.8 pF, respectively, on account of the additional capacitance between the cap and the antenna. If we neglect the slight changes in the capacitance, each conductance in the circuit can be separated into G_{Rn} and G_{Ln}. The antenna efficiency can then be easily calculated from (7).

In Fig. 4(a), the radiation efficiency using the circuit model is represented by a solid line, and the simulated efficiency from the IE3D EM simulator is shown by a dotted line. The measured efficiencies from the Wheeler cap method with a series-(or parallel-) resonant circuit model are also represented in the figure using dotted lines for the values obtained from comparing resistances, and dash-dotted lines for the values obtained from comparing conductances [7], [9]. The modified procedure using the high-order circuit yields results that are close to the

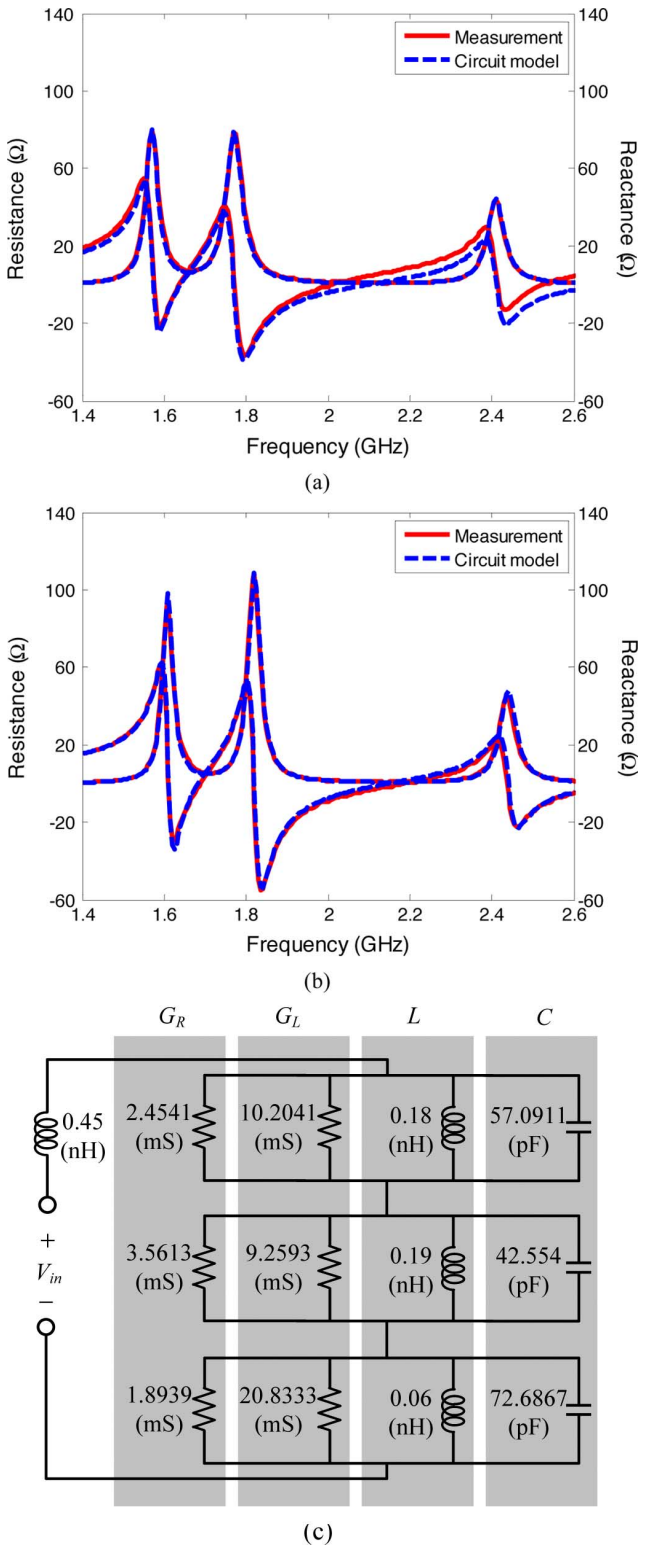

Fig. 6. Calculated impedance of the equivalent circuit (- - - - -) and measured impedance (——) for the miniaturized multi-resonance antenna (a) in free space and (b) the cap, and (c) the equivalent circuit model.

simulated values, whereas the Wheeler cap method with a series-(or parallel-) resonant circuit model produces unreliable results near the resonant frequencies. The solid line in Fig. 4(b) shows the percentage error between the measured efficiency from the proposed technique and the simulated efficiency. The error is less than 5% in the operating frequency range of 880 to 920 MHz. The dashed line represents the percentage error between the impedance of our circuit model and the measured values, and this error is less than 10% at operating frequency. The efficiency measurements become more accurate when the impedance of the circuit model is close to the measured impedance. This result indicates that we can obtain more accurate radiation-efficiency measurements using a modified Wheeler cap method with a more precise circuit model.

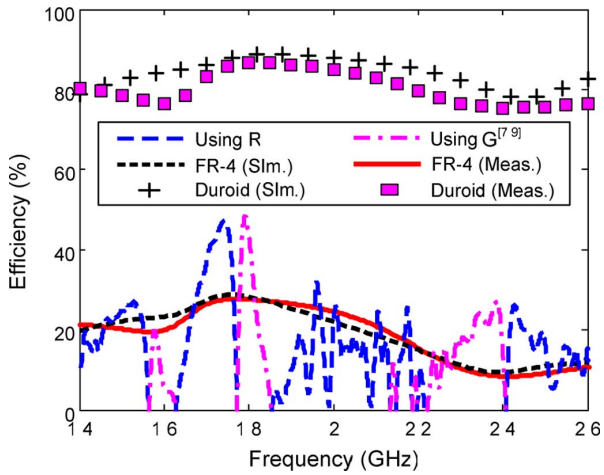

Fig. 7. Efficiency results for the miniaturized multi-resonance antenna measured by the proposed method when the patch is printed on the FR-4 substrate (——) and Duroid substrate (■), measured by the conventional Wheeler cap method using R comparison (- - - - -) and G comparison (—·—·—), and the simulated result on the FR-4 substrate (· · · · · · · ·) and Duroid (+) substrate.

B. Efficiency of a Miniaturized Patch Antenna With Multi-Resonances

Next we apply our procedure to measure the efficiency of a miniaturized triple-band patch antenna [15]. The patch is printed on the same FR-4 substrate as the CP patch antenna discussed in the previous section. Fig. 5 shows the measured reflection coefficient, with resonant peaks at 1.6, 1.8, and 2.4 GHz. In this case, we use three parallel circuits ($N = 3$) to model the three resonances. As with the CP patch antenna, we use (8) to reduce the number of unknown lumped element values. The impedances of the circuit model are fairly well matched with actual measurements in the entire frequency band from 1.4–2.6 GHz, as shown in Fig. 6(a). When the Wheeler cap is placed on the antenna, the impedance response of the circuit model remains in close agreement with the measurements, as shown in Fig. 6(b). Using the lumped element values from Fig. 6(a) and (b), we construct the full circuit model of the triple-band patch antenna, as illustrated in Fig. 6(c). Since the antenna is printed on a very lossy dielectric substrate, the loss conductances are much larger than the radiation conductances in this circuit.

The efficiency is calculated from (7), and the results are represented by the solid line in Fig. 7. They are in close agreement with the simulated results (dotted line), whereas the efficiency measurements using the Wheeler cap method with a series-(or parallel-) resonant circuit model is oscillatory and unreliable. Although low-cost fabrication of patch antennas can be readily accomplished with the FR-4 substrate, the resulting efficiency is usually very low (less than 30%). Hence, the engineer might find it preferable to use a low-loss substrate material despite its higher cost.

Accordingly, we also validated our technique for a patch antenna printed on a very low-loss dielectric substrate. We printed the same triple-band patch antenna on a Duroid 5880 substrate ($\varepsilon_r = 2.2, \tan\delta = 0.0009$) and again measured the radiation efficiency. To obtain a fair comparison, we magnified the size of the patch

by a factor of 1.35 to preserve the resonant frequencies of 1.6, 1.8, and 2.4 GHz (see Fig. 5). The measured efficiency ("□") is once again in close agreement with the simulation ("+") and increases by a factor of roughly four compared to the antenna printed on the FR-4 substrate. These results indicate that the proposed procedure provides a better estimate of the radiation efficiency for a probe-fed patch antenna with multiple resonances. We also applied the proposed method to other types of antennas such as RFID tags, planar dipoles, and electrically small antennas with multi-resonances. They also had good results when a built circuit model clearly represented the antennas' operation.

IV. Conclusion

To obtain more accurate radiation-efficiency measurements, we introduced a high-order circuit model into the Wheeler cap method. The radiation efficiency is calculated from the power consumption ratios of the radiation and loss conductances. To validate our technique, we measured the radiation efficiency of a microstrip antenna with circularly polarized radiation and a miniaturized triple-band patch antenna. The measured results became more accurate when the impedance of the circuit model was close to the measured impedance, whereas Wheeler cap method with a series-(or parallel-) resonant circuit model produced unreliable results. These findings demonstrate that we can obtain more accurate radiation-efficiency measurements by using the Wheeler cap method with a more precise circuit model.

References

[1] S. D. Rogers, J. T. Aberle, and D. T. Auckland, "Two-port model of an antenna for use in characterizing wireless communications systems, obtained using efficiency measurements," *IEEE Antennas Propag. Mag.*, vol. 45, no. 3, pp. 115–118, Jun. 2003.

[2] A. Khaleghi, "Time-domain measurement of antenna efficiency in reverberation chamber," *IEEE Trans. Antennas Propag.*, vol. 57, no. 3, pp. 817–821, Mar. 2009.

[3] W. L. Schroeder and D. Gapski, "Direct measurement of small antenna radiation efficiency by calorimetric method," *IEEE Trans. Antennas Propag.*, vol. 54, no. 9, pp. 2646–2656, Sep. 2006.

[4] H. Wheeler, "The radiansphere around a small antenna," *Proc. IRE*, vol. 47, no. 8, pp. 1325–1331, Aug. 1959.

[5] E. Newman, P. Bohley, and C. Walter, "Two methods for the measurement of antenna efficiency," *IEEE Trans. Antennas Propag.*, vol. 23, no. 4, pp. 457–461, Jul. 1975.

[6] G. Smith, "An analysis of the Wheeler method for measuring the radiating efficiency of antennas," *IEEE Trans. Antennas Propag.*, vol. 25, no. 4, pp. 552–556, Jul. 1977.

[7] D. M. Pozar and B. Kaufman, "Comparison of three methods for the measurement of printed antenna efficiency," *IEEE Trans. Antennas Propag.*, vol. 36, no. 1, pp. 136–139, Jan. 1988.

[8] R. H. Johnston and J. G. McRory, "An improved small antenna radiation-efficiency measurement method," *IEEE Antennas Propag. Mag.*, vol. 40, no. 5, pp. 40–48, Oct. 1998.

[9] H. Choo, R. Rogers, and H. Ling, "On the Wheeler cap measurement of the efficiency of microstrip antennas," *IEEE Trans. Antennas Propag.*, vol. 53, no. 7, pp. 2328–2332, Jul. 2005.

[10] A. Galehdar, D. V. Thiel, and S. G. O'Keefe, "Antenna efficiency calculations for electrically small, RFID antennas," *IEEE Antennas Wireless Propag. Lett.*, vol. 6, no. 11, pp. 156–159, 2007.

[11] W. Richards, Y. Lo, and D. Harrison, "An improved theory for microstrip antennas and application," *IEEE Trans. Antennas Propag.*, vol. 29, no. 1, pp. 38–46, Jan. 1981.

[12] D. M. Pozar, "Microstrip antennas," *Proc. IEEE*, vol. 80, no. 1, pp. 79–91, Jan. 1992.

[13] R. Garg, P. Bhartia, I. Bahl, and A. Ittipiboon, *Microstrip Antenna Design Handbook*. Norwood, MA: Artech House, 2001.

[14] *IE3D Ver.12.0*, [Online]. Available: www.Zealand.com.

[15] H. Choo and H. Ling, "Design of multiband microstrip antennas using a genetic algorithm," *IEEE Microw. Wireless Compon. Lett.*, vol. 12, no. 9, pp. 345–347, Sep. 2002.

On the Accuracy of Three Different Six Stages SS-FDTD Methods for Modeling Narrow-Band Electromagnetic Applications

Omar Ramadan

***Abstract*—Recently, three different six stages split-step finite difference time domain (SS-FDTD) methods introduced for removing the FDTD Courant-Friedrichs-Levy (CFL) stability limit. Accuracy performance of these methods for modeling narrow-band electromagnetic applications is studied. Numerical example carried out in two-dimensional domain shows that when the CFL stability limit is exceeded, the accuracy of the classical FDTD scheme is maintained only with the splitting scheme that solves the field equations at each FDTD sub-stage alternatively between the x and y directions.**

***Index Terms*—Complex envelope finite difference time domain, split-step approach.**

I. Introduction

Recently, three different unconditionally stable split-step six stages finite difference time domain (SS6-FDTD) methods have been introduced for solving two-dimensional (2D) broad-band electromagnetic applications [1]. These methods are based on splitting each FDTD time step (Δ_t) into six sub-stages with an equal time increment of $\Delta_t/6$ and then solving the field equations at each sub-stage along one direction only. In the first method, referred as SS6-1-FDTD, the Maxwell's matrix equations are split into sub-matrices in which the field equations are solved alternatively between x and y directions. The second (SS6-2-FDTD) and the third (SS6-3-FDTD) splitting methods are deduced by adjusting the sequence of the sub-matrices to be solved at each sub-stage. It has been reported in [1] that these methods not only remove the FDTD Courant-Friedrichs-Levy (CFL) stability limit but also can provide better accuracy with less computational requirements as compared with other FDTD splitting techniques.

In this communication, the accuracy performance of the SS6-FDTD methods for modeling narrow-band electromagnetic applications is studied. In the presented study, the complex envelope FDTD (CE-FDTD) [2] scheme is incorporated with the SS6-FDTD formulations of [1]. Numerical example carried out in 2D domain shows that when the SS6-FDTD methods are used for modeling band-limited electromagnetic applications, only the CE-SS6-1-FDTD scheme, which alternatively solves the field equations between x and y directions, maintains the accuracy of the conventional CE-FDTD scheme with a considerable decrease in the CPU time while the accuracy of the other splitting methods decreases rapidly as the time step exceeds the CFL stability limit.

Manuscript received December 15, 2009; revised February 23, 2010, March 21, 2010; accepted March 23, 2010. Date of publication June 14, 2010; date of current version September 03, 2010.

The author is with the Computer Engineering Department, Eastern Mediterranean University, Gazi Magusa, Mersin 10, Turkey (e-mail: omar.ramadan@emu.edu.tr).

Color versions of one or more of the figures in this communication are available online at http://ieeexplore.ieee.org.

Digital Object Identifier 10.1109/TAP.2010.2052580